THE JOURNAL OF BIOLOGICAL CHEMISTRY VOL. 281, NO. 30, pp. 21469–21479, July 28, 2006
Printed in the U.S.A.

# Multiple Conformations of Phosphodiesterase-5

## *IMPLICATIONS FOR ENZYME FUNCTION AND DRUG DEVELOPMENT**

Received for publication, November 22, 2005, and in revised form, May 18, 2006 Published, JBC Papers in Press, May 30, 2006, DOI 10.1074/jbc.M512527200

**Huanchen Wang[‡], Yudong Liu[‡], Qing Huai[‡1], Jiwen Cai[‡§], Roya Zoraghi[¶], Sharron H. Francis[¶], Jackie D. Corbin[¶], Howard Robinson[‖], Zhongcheng Xin[**], Guiting Lin[‡‡], and Hengming Ke[‡2]**

*From the [‡]Department of Biochemistry and Biophysics and Lineberger Comprehensive Cancer Center, University of North Carolina, Chapel Hill, North Carolina 27599-7260, [§]School of Pharmaceutical Sciences, Sun Yat-sen University, Guangzhou, 510080, China, the [¶]Department of Molecular Physiology and Biophysics, Vanderbilt University School of Medicine, Nashville, Tennessee 37232-0615, [‖]Biology Department, Brookhaven National Laboratory, Upton, New York 11973-5000, [**]Andrology Center, Peking University First Hospital, Peking University, 8 Xishiku Street, Beijing (100034), China, and the [‡‡]Department of Urology, University of California, San Francisco, California 94143-1695*

**Phosphodiesterase-5 (PDE5) is the target for sildenafil, vardenafil, and tadalafil, which are drugs for treatment of erectile dysfunction and pulmonary hypertension. We report here the crystal structures of a fully active catalytic domain of unliganded PDE5A1 and its complexes with sildenafil or icarisid II. These structures together with the PDE5A1-isobutyl-1-methylxanthine complex show that the H-loop (residues 660–683) at the active site of PDE5A1 has four different conformations and migrates 7–35 Å upon inhibitor binding. In addition, the conformation of sildenafil reported herein differs significantly from those in the previous structures of chimerically hybridized or almost inactive PDE5. Mutagenesis and kinetic analyses confirm that the H-loop is particularly important for substrate recognition and that invariant Gly[659], which immediately precedes the H-loop, is critical for optimal substrate affinity and catalytic activity.**

Cyclic nucleotide phosphodiesterases (PDEs)[3] are key enzymes controlling cellular concentrations of second messengers cAMP and cGMP by hydrolyzing them to 5′-AMP and 5′-GMP, respectively. The human genome encodes 21 PDE genes that are categorized into 11 families (1–9). Alternative mRNA splicing of the PDE genes produces over 60 PDE isoforms that distribute in various cellular compartments and control physiological processes. PDE molecules contain a conserved catalytic domain and variable regulatory regions. However, each PDE family possesses a characteristic pattern of substrate specificity and inhibitor selectivity (6).

Inhibitors of PDEs have been widely studied as therapeutics as follows: cardiotonics, vasodilators, smooth muscle relaxants, antidepressants, antithrombotics, antiasthmatics, and agents for improving cognitive functions such as learning and memory (10–17). Some of the most successful examples of these drugs are the PDE5 inhibitors sildenafil (Viagra®), vardenafil (Levitra®), and tadalafil (Cialis®) that have been used for treatment of male erectile dysfunction (15). Sildenafil has also recently been approved (Revatio®) for treatment of pulmonary hypertension (18). However, reported side effects of these medications such as headache and visual disturbance suggest a need for further study of the molecular basis of the selectivity of PDE5 inhibitors (19).

Two co-crystal structures of the catalytic domain of PDE5 with sildenafil showed differences in the conformation of the inhibitor bound to the catalytic site (20–22). However, it remains unknown whether these conformations are biologically relevant because the PDE5 enzyme used in the studies is either almost inactive (20) or a chimeric hybrid of the PDE5 catalytic domain with replacement of a PDE4 segment (the H-loop) (21, 22). In addition, the crystal structure of the catalytic domain of PDE5A1 in complex with the nonselective PDE inhibitor 3-isobutyl-1-methylxanthine (IBMX) showed that the conformation of the H-loop at the active site is different from that in PDE4 (23) and in other published PDE5 structures (20–22, 24). We report here the structure of the catalytic domain of human PDE5A1 in the unliganded state, as well as the structures of the protein in complex with inhibitors sildenafil and icarisid II (Fig. 1). These structures, together with that of PDE5A1-IBMX, reveal four different conformations of the H-loop, which is juxtaposed to the catalytic pocket of the enzyme. In addition, comparison of this PDE5-sildenafil structure with the previously published structures shows significantly different conformations of the methylpiperazine portion of sildenafil. These unique features of the PDE5 catalytic domain and the sildenafil configuration are key considerations for understanding the action of sildenafil and for development of PDE5 inhibitors.

## EXPERIMENTAL PROCEDURES

*Protein Expression and Purification of Catalytic Domain PDE5A1*—The cDNA of the catalytic domain of human PDE5A1 was generated by site-directed mutagenesis of the bovine PDE5A cDNA (23). The coding regions for amino acids 535–860 of PDE5A1 were amplified by PCR and sub-

* This work was supported in part by National Institutes of Health Grants GM59791 (to H. K.), DK58277, and DK40029 (to J. C.), and American Heart Association Postdoctoral Fellowship 032525B (to R. Z.). The costs of publication of this article were defrayed in part by the payment of page charges. This article must therefore be hereby marked "*advertisement*" in accordance with 18 U.S.C. Section 1734 solely to indicate this fact.

*The atomic coordinates and structure factors (codes 2H40, 2H42, and 2H44) have been deposited in the Protein Data Bank, Research Collaboratory for Structural Bioinformatics, Rutgers University, New Brunswick, NJ (http://www.rcsb.org/).*

[1] Present address: Center for Homeostasis and Thrombosis Research, Beth Israel Deaconess Medical Center and Dept. of Medicine, Harvard Medical School, 41 Ave. Louis Pasteur, Boston, MA 02115.

[2] To whom correspondence should be addressed. Tel.: 919-966-2244; Fax: 919-966-2852; E-mail: hke@med.unc.edu.

[3] The abbreviations used are: PDEs, phosphodiesterases; IBMX, 3-isobutyl-1-methylxanthine; r.m.s., root mean square.

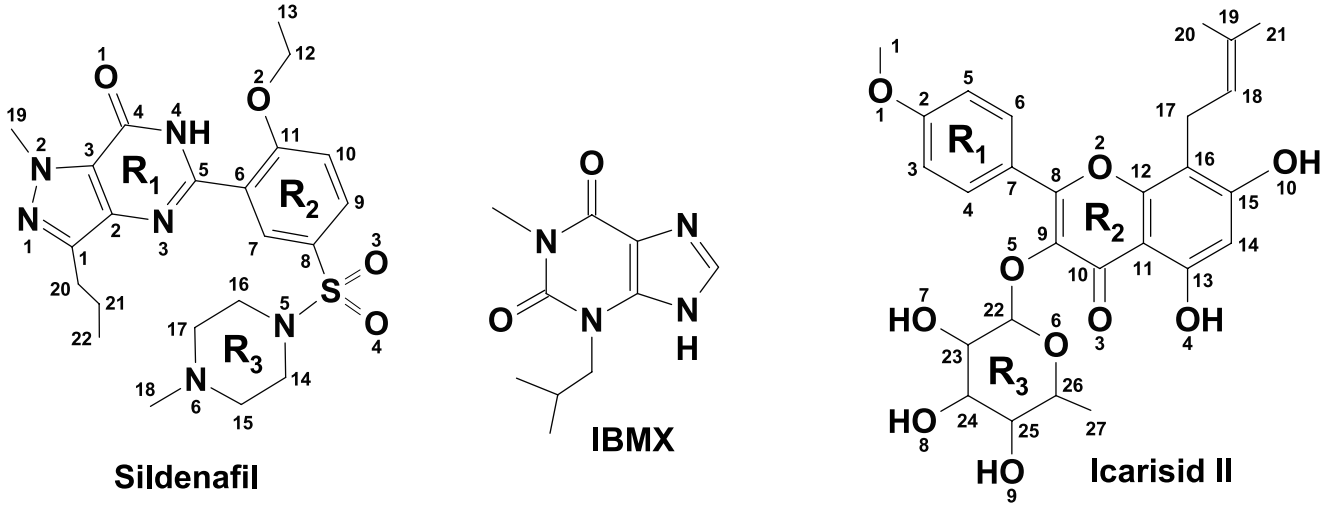


FIGURE 1. **Chemical structures of PDE5 inhibitors.** The letters $R_1$–$R_3$ label the main groups in sildenafil and icarisid II. In sildenafil, $R_1$ represents the pyrazolopyrimidinone group; $R_2$ is ethoxyphenyl, and $R_3$ is methylpiperazine. In icarisid II, $R_1$ represents the methoxyphenyl group; $R_2$ is oxychromone, and $R_3$ is rhamnose.

cloned into the expression vector pET15b. The resultant plasmid pET-PDE5A1 was transferred into *Escherichia coli* strain BL21 (Codonplus) for overexpression. The *E. coli* cell carrying pET-PDE5A1 was grown in LB medium at 37 °C to an $A_{600} = 0.7$, and 0.1 mM isopropyl β-D-thiogalactopyranoside was then added for further growth at 15 °C overnight. Recombinant PDE5A1 was purified by the columns of nickel-nitrilotriacetic acid (Qiagen), Q-Sepharose, and Sephacryl S300 (Amersham Biosciences). A typical purification yielded over 10 mg of PDE5A1 with a purity of >95% from a 2-liter cell culture.

The mutant proteins with deletion of residues 663–678 and 661–681 were produced by the standard protocol of site-directed mutagenesis. For the deletion mutant proteins, four glycine residues were inserted as the spacer to minimize the disturbance on the three-dimensional structure. Overexpression and purification of the mutant proteins used the same protocols as for the nonmutated protein.

*Expression and Purification of Full-length hPDE5A1*—Human cDNA coding for full-length PDE5A1 was cloned into pCR 2.1-TOPO® vector (Invitrogen) and then ligated into the baculovirus expression vector pAcHLT-A (Pharmingen). The resulting plasmid pAcA-PDE5 ($Met^1$–$Asn^{875}$) was used to make point mutations (G659A, V660Q, N661A, N662A, Y664A, H678A, and S679A) with the QuikChange site-directed mutagenesis kit (Stratagene). Wild type and mutant constructs of hPDE5A1 were expressed in Sf9 cells. Sf9 cells were cotransfected with BaculoGold linear baculovirus DNA (Pharmingen) and one of the pAcA-hPDE5A1 plasmids. The cotransfection supernatant was collected at 5 days post-infection, amplified three times in Sf9 cells, and then used directly as virus stock without additional purification. Sf9 cells grown at 27 °C in complete Grace's insect medium with 10% fetal bovine serum and 10 μg/ml gentamicin (Sigma) were typically infected with 100 μl of viral stock and then harvested at 92 h post-infection. Protein yields were ~2.7 mg/liter infected cell media and were largely soluble.

The Sf9 cell pellet (~$2 \times 10^7$ cells) was resuspended in ice-cold lysis buffer (20 mM Tris-HCl, pH 8, 100 mM NaCl) containing protease inhibitor mixture, homogenized, and centrifuged. The supernatant was loaded onto a nickel-nitrilotriacetic acid-agarose (Qiagen) column equilibrated with lysis buffer. The column was washed with lysis buffer containing a stepwise gradient of 0.8–20 mM imidazole and eluted with 100 mM imidazole. Eluted PDE5A1 protein was dialyzed *versus* 2000 volumes of ice-cold 10 mM potassium phosphate, pH 6.8, 25 mM β-mercaptoethanol, and 150 mM NaCl. All recombinant PDE5A1 proteins exhibited a purity of >98% as determined by SDS-PAGE.

*Enzymatic Assay*—Enzymatic activity of the isolated catalytic domains of wild type PDE5A1 and its deletion mutants was assayed by using [$^3$H]cGMP as substrate in a reaction mixture of 20 mM Tris-HCl, pH 7.8, 1.5 mM dithiothreitol, 10 mM $MgCl_2$, [$^3$H]cGMP (40,000 cpm/assay) at 24 °C for 15 min (25). The reaction was terminated by addition of 0.2 M $ZnSO_4$ and $Ba(OH)_2$. Radioactivity of unreacted [$^3$H]cGMP in the supernatant was measured by a liquid scintillation counter. The turnover rate was measured at nine concentrations of cGMP and controlled at hydrolysis of 15–40% substrate. Each measurement was repeated three times. For measurement of $IC_{50}$ values, 10 concentrations of inhibitors were used at a substrate concentration that was one-tenth of the $K_m$ value and an enzyme concentration that hydrolyzed 50% of substrate.

To assay the activity of full-length hPDE5A1, the reaction mixture contained 50 mM Tris-HCl, pH 7.5, 10 mM $MgCl_2$, 0.3 mg/ml bovine serum albumin, 0.05–250 μM cGMP, and [$^3$H]cGMP (100,000–150,000 cpm/assay) and one of the PDE5A1 proteins (26). Incubation time was 10 min at 30 °C. In all studies, less than 10% of total [$^3$H]cGMP was hydrolyzed during the reaction. All values determined represent three measurements. The $K_m$ and $k_{cat}$ values for cGMP were determined by nonlinear regression analysis of data using Prism GraphPad software.

*Crystallization and Data Collection*—All crystals of PDE5A1-(535–860) were grown by vapor diffusion. The pro-

**TABLE 1**
**Statistics on diffraction data and structure refinement**

| Data collection | PDE5A1 native | PDE5A1-sildenafil | PDE5A1-icarisid II |
|---|---|---|---|
| Space group | $P3_121$ | $P6_222$ | $P6_122$ |
| Unit cell (*a*, *b*, and *c*, Å) | 74.7, 74.7, 130.7 | 164.6, 164.6, 193.1 | 110.7, 110.7, 106.2 |
| Resolution (Å) | 1.85 | 2.3 | 1.8 |
| Total measurements | 363,960 | 1,121,219 | 412,999 |
| Unique reflections | 36,603 | 68,786 | 36,177 |
| Completeness (%) | 99.5 (100.0)[a] | 99.9 (100.0) | 99.9 (99.7) |
| Average $I/\sigma$ | 20.8 (7.4)[a] | 6.7 (4.8) | 13.6 (4.3) |
| $R_{merge}$ | 0.058 (0.49)[a] | 0.117 (0.58) | 0.061 (0.46) |
| **Structure refinement** | | | |
| *R*-factor | 0.221 | 0.210 | 0.206 |
| *R*-free | 0.236 (9.7%)[b] | 0.246 (9.7%) | 0.233 (9.7%) |
| Resolution (Å) | 15–1.85 | 48–2.3 | 44–1.8 |
| Reflections | 34,996 | 66,315 | 35,094 |
| **r.m.s. deviation** | | | |
| Bond | 0.0078 Å | 0.0061 | 0.0073 |
| Angle | 1.25° | 1.17° | 1.31° |
| **Average *B*-factor (Å$^2$)** | | | |
| Protein | 37.5 (2523)[c] | 27.8 (7804) | 27.9 (2650) |
| Inhibitor | | 29.4 (99) | 25.9 (37) |
| Water | 37.9 (148)[c] | 28.8 (311) | 32.8 (231) |
| Zinc | 46.2 (1)[c] | 44.9 (3) | 36.6 (1) |
| Magnesium | 33.4 (1)[c] | 37.6 (3) | 41.0 (1) |

[a] The numbers in parentheses are for the highest resolution shell.
[b] The percentage of reflections omitted for calculation of *R*-free.
[c] The number of atoms in the crystallographic asymmetric unit.

tein drop was prepared by mixing 2 $\mu$l of protein with 2 $\mu$l of well buffer. The unliganded PDE5A1 crystal was grown at room temperature against well buffer of 0.2 M $MgSO_4$, 0.1 M Tris base, pH 8.5, 12% PEG 3350, and 2% ethanol. The PDE5A1-sildenafil complex was prepared by mixing 1 mM sildenafil with 15 mg/ml PDE5A1 at 4 °C overnight and crystallized against a well buffer of 1.0 M sodium citrate, 2.5% ethanol, 0.1 M HEPES, pH 7.5, at 4 °C. The PDE5A1-icarisid II complex was prepared by mixing 2 mM icarisid II with 15 mg/ml protein at 4 °C overnight, and crystallized against a well buffer of 0.1 M HEPES, pH 7.5, 12% PEG3350 at room temperature.

The unliganded PDE5A1-(535–860) was crystallized in the space group $P3_121$ with cell dimensions of $a = b = 74.7$ and $c = 130.7$ Å. The PDE5A1-sildenafil crystal had the space group $P6_222$ with cell dimensions of $a = b = 164.6$ and $c = 193.1$ Å. The PDE5A1-icarisid II crystal had the space group $P6_122$ with cell dimensions of $a = b = 110.7$ and $c = 106.2$ Å. Beamline X25 at Brookhaven National Laboratory was used for collection of diffraction data of the unliganded PDE5A1 and X29 for PDE5A1-sildenafil and PDE5A1-icarisid II (Table 1). All data were processed by the program HKL (27).

*Structure Determination*—The structure of the unliganded PDE5A1 was solved by rigid body refinement of the PDE5A1 catalytic domain in PDE5A1-IBMX. The structures of PDE5A1 in complex with sildenafil and icarisid II were solved by the molecular replacement program AMoRe (28), using the PDE5A1-IBMX structure without the H-loop and IBMX as the initial model. The rotation and translation searches for the crystal of PDE5A1-icarisid II yielded a correlation coefficient of 0.74 and *R*-factor of 0.31 for 3054 reflections between 4 and 8 Å resolution. The rotation and translation searches for PDE5A1-sildenafil yielded a correlation coefficient of 0.22 and *R*-factor of 0.52 for 11,612 reflections between 4 and 8 Å resolution for the first molecule, and of 0.39 and 0.41 after the second molecule was added. The electron density map was improved by the density modification package of CCP4 (29). The atomic model was rebuilt by program O (30) and refined by program CNS (Table 1) (31).

## RESULTS

*Multiple Conformations of the H-loop of PDE5*—The crystallographic asymmetric units contain one molecule of the catalytic domain in the structures of the unliganded PDE5A1 and the icarisid II complex but three molecules in PDE5A1-sildenafil structure. The electron density maps showed that the entire catalytic domain in the PDE5A1-icarisid II structure and molecule A in the PDE5A1-sildenafil structure were traceable. However, residues 668–676 of molecules B and C in the PDE5A1-sildenafil crystal and residues 793–807 in the unliganded PDE5A1 lacked electron density and were disordered. The Ramachandran plots showed that the backbone conformations of 90–94% residues in the three structures were located in the most favored regions, and no residues were located in the energetically disallowed regions.

The structures of the unliganded PDE5A1 catalytic domain (residues 535–860) and its complexes with sildenafil or icarisid II are composed of 14 common $\alpha$-helices and a variable H-loop at the active site (Fig. 2). Structural superposition of the unliganded PDE5A1 over the complexes of PDE5A1-IBMX, PDE5A1-sildenafil, and PDE5A1-icarisid II yielded r.m.s. deviations of 0.29, 0.42, and 0.54 Å for the C$\alpha$ atoms of comparable residues (536–659, 684–787, and 810–860), respectively, suggesting overall structural similarity. However, the H-loop (residues 660–683 on the basis of the structural comparison with seven other PDE families, which are slightly different from the previous assignment of residues 661–676 (23)) adopts four conformations and different tertiary structures in the crystals of the unliganded PDE5A1 and its complexes with IBMX, sildenafil, or icarisid II. In the unliganded PDE5A1 structure, the H-loop contains a few turns, but the majority of the H-loop

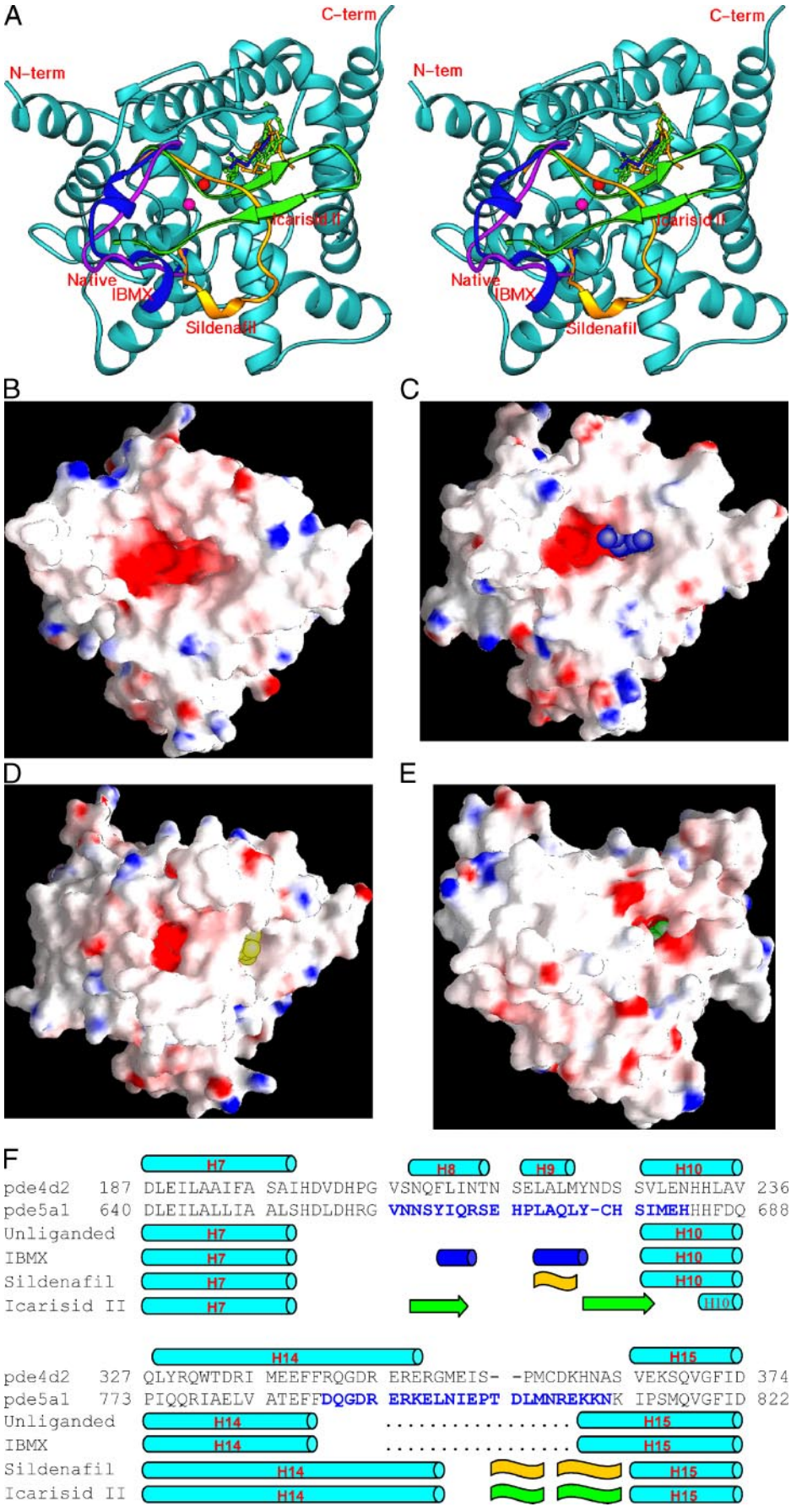
A
C-term
N-term
Native
IBMX
Sildenafil
C-term
N-tem
Native
IBMX
Sildenafil
B
C
D
E
F
H7
H8
H9
H10
pde4d2 187 DLEILAAIFA SAIHDVDHPG VSNQFLINTN SELALMYNDS SVLENHHLAV 236
pde5a1 640 DLEILALLIA ALSHDLDHRG VNNSYIQRSE HPLAQLY-CH SIMEHHHFDQ 688
Unliganded
IBMX
Sildenafil
Icarisid II
H14
H15
pde4d2 327 QLYRQWTDRI MEEFFRQGDR ERERGMEIS- -PMCDKHNAS VEKSQVGFID 374
pde5a1 773 PIQQRIAELV ATEFFDQGDR ERKELNIEPT DLMNREKKNK IPSMQVGFID 822
Unliganded
IBMX
Sildenafil
Icarisid II

residues are in a coil conformation (Fig. 2). Binding of IBMX converts the H-loop into two short α-helices involving residues 664–667 and 672–676 (Fig. 2*F*) and shifts the Cα atoms of the H-loop as much as 7 Å from those in the unliganded structure. In the structure of the PDE5-sildenafil complex, the H-loop in molecule A is converted to a turn and a $3_{10}$ helix at residues 672–675, and the whole loop migrates as much as 24 Å to cover the active site (Fig. 2). However, residues 668–676 of the H-loop in molecules B and C are disordered. The most dramatic change in the H-loop occurs in the structure of PDE5A1-icarisid II, in which the H-loop contains two β-strands at residues 662–666 and 675–679 (Fig. 2*F*) and migrates as much as 35 Å from the position in the unliganded PDE5A1.

To verify that the conformational changes are not because of an artifact of structure determination or crystal packing, electron density maps were calculated, and lattice interactions in the various crystal forms were examined. The maps that were calculated from the structure with omission of the H-loop showed solid electron density for almost all residues of the H-loops, thus confirming the true conformational variation in the PDE5A1 structures. This is supported by the fact that the *B*-factor for the H-loops is comparable with or slightly higher than the overall average *B*-factor for the protein atoms as follows: 48 *versus* 38 Å$^2$ for the unliganded PDE5A1, 61 *versus* 40 Å$^2$ for PDE5A1-IBMX, 33 *versus* 33 Å$^2$ for PDE5A1-icarisid II, and 38 *versus* 27 Å$^2$ for PDE5A1-sildenafil. In addition, the following facts suggest minor roles of the lattice contacts in the conformational changes of the H-loop. First, the unliganded PDE5A1 and its IBMX complex have the same space group and the similar unit cell parameters ($a = b = 74.7$, $c = 130.7$ Å *versus* $a = b = 74.5$, $c = 130.1$ Å) but different H-loop conformations. Second, the PDE4 H-loop that was inserted into the chimeric PDE5 structure is involved in the crystal lattice interactions of PDE5 but retains its conformation found in PDE4 (22). Thus, the dramatic conformational changes of the H-loop must be the consequence of binding of the specific inhibitors.

In addition to variation of the H-loop, minor conformational differences are observed for another active site loop, the M-loop (residues 788–811 on the basis of the structural comparison among seven PDE families, in comparison to the original assignment of residues 787–812 (23)). Residues 793–807 of the M-loop are not traceable in the structures of the unliganded or IBMX-bound PDE5A1. However, the well ordered M-loops in the structures of PDE5A1 in complex with sildenafil or icarisid II contain an extra $3_{10}$ helix and a 10-residue extension of α-helix H14, in addition to the correspondence of a $3_{10}$ helix to the N-terminal portion of H15 in the unliganded PDE5A1 (Fig. 2*F*).

PDE5 shows an apparently unique feature distinct from other PDE families, although the overall topological folding of PDE5A is similar to those of PDE1B (22), PDE2A (32), PDE3B (33), PDE4B and PDE4D (22–24, 34–38), PDE7A (25), and PDE9A (39). The core catalytic domains of PDE1–4, -7, and -9 (residues 115–411 in PDE4D2), including the H-loop that is composed of two short α-helices (H8 and H9, residues 209–215 and 218–222 in PDE4D2l; see Fig. 2*F*) have a uniform conformation and are superimposable on one another. In contrast, the H-loop of PDE5A1 presents at least four different conformations, and none of these is comparable with any of the corresponding H-loops in other PDE families. The closest comparable conformation is the H-loop in the PDE5A1-IBMX structure, which also contains two short α-helices. However, these two helices have as much as 7 Å positional difference from those in PDE4D2 (23) and are in a different three-dimensional arrangement. In addition, the β-strand component of the H-loop in the PDE5A1-icarisid II complex is unique among active sites of known PDE structures. Therefore, the active site of PDE5 appears to belong to a special category of the PDE superfamily.

*Conformation Variation of Sildenafil*—Sildenafil binds to each active site of three PDE5A1 catalytic domains in the crystallographic asymmetric unit with similar conformation and occupancy, as shown by the comparable *B*-factor and the clean electron density in the omitted map (Fig. 3). The binding of sildenafil causes a dramatic conformational change of the H-loop and a movement as much as 24 Å from that in the unliganded PDE5 structure. A direct consequence of the H-loop movement is the transformation of the open PDE5A1 active site to a closed pocket. Sildenafil is partially buried in the pocket. Solvent-accessible surface of sildenafil after binding to PDE5A1 is reduced to 9.4% of the total surface area. Sildenafil borders the metal-binding pocket but does not directly interact with the metal ions. The pyrazolopyrimidinone group ($R_1$ in Fig. 1 and Table 2) of sildenafil stacks against Phe$^{820}$ of PDE5A1 and also contacts residues Tyr$^{612}$, Leu$^{765}$, Ala$^{767}$, and Gln$^{817}$. The O1 and N4 atoms of pyrazolopyrimidinone form two hydrogen bonds with Nϵ2 and Oϵ1 of Gln$^{817}$, respectively. The ethoxyphenyl group ($R_2$, Fig. 1) interacts via van der Waals forces with Val$^{782}$, Ala$^{783}$, Phe$^{786}$, Leu$^{804}$, Ile$^{813}$, Gln$^{817}$, and Phe$^{820}$. The methylpiperazine group ($R_3$, Fig. 1) contacts Asn$^{662}$, Ser$^{663}$, Tyr$^{664}$, Ile$^{665}$, Leu$^{804}$, and Phe$^{820}$. The oxygen atoms of the sulfone group interact mainly with Phe$^{820}$.

Our PDE5A1-sildenafil structure is similar in many respects to those reported earlier (20–22), as shown by the r.m.s. deviations of 0.59 and 0.40 Å for superposition of the backbone atoms of the comparable residues (without 661–677) of our PDE5A1-sildenafil over the two previous structures. However, two significant differences are observed among the three PDE5A-sildenafil structures. First, the H-loop in our structure has definite electron density and different conformation from those in the previously published structures in which the H-loop is either disordered (missing residues 665–675) (20) or

FIGURE 2. **Structures of PDE5 and its inhibitor complexes.** *A,* ribbon diagram. The *cyan ribbons* are the common structures of the catalytic domains of unliganded PDE5A1 and its complexes. The different conformations of the H-loop in the four structures are shown in *purple* for the unliganded PDE5A1, *blue* for the IBMX complex, *gold* for the sildenafil complex, and *green* for the icarisid II complex. Zinc is colored *red,* and magnesium is *purple. B–E,* surface presentation for the catalytic domain of the unliganded PDE5A1 (*B*) and its complexes with IBMX (*C*), sildenafil (*D*), or icarisid II (*E*). The *middle red pocket* is the active site. The inhibitors are shown as color balls: *blue* for IBMX, *gold* for sildenafil, and *green* for icarisid II. Icarisid II is almost completely buried, and the orientation of the domain is adjusted to show the icarisid II binding. *F,* the alignment of the secondary structures with the amino acid sequence around the regions of the H- and M-loops that are shown in *blue letters.* The *gold ribbon*, *green arrow*, and *cyan tube* represent $3_{10}$ helix, β-strand, and α-helix, respectively. The *dots* represent disordered regions in the unliganded and IBMX-bound PDE5.

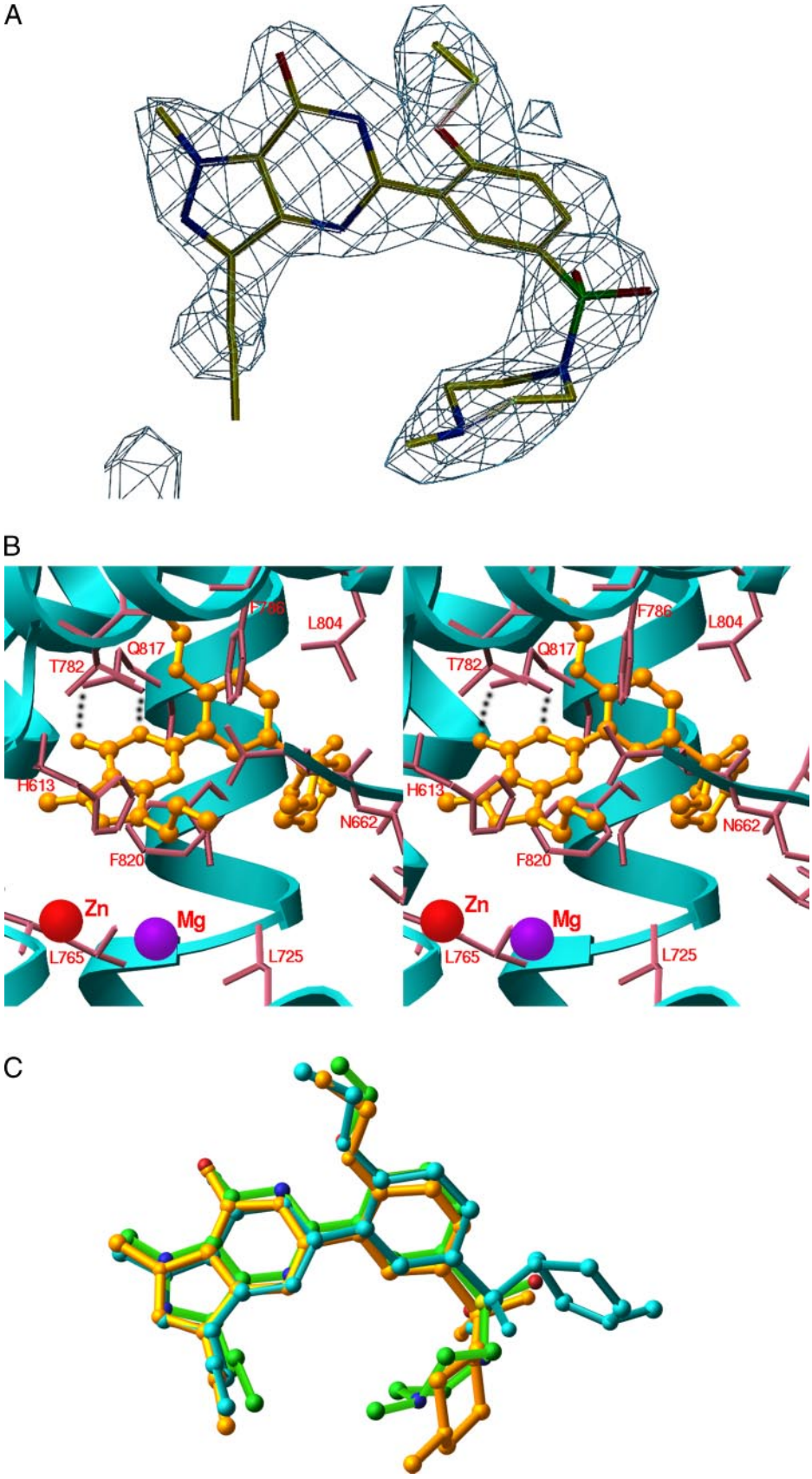


FIGURE 3. **Sildenafil binding.** *A,* electron density for sildenafil bound to PDE5A1. The $F_o - F_c$ map was calculated from the structure omitting sildenafil and contoured at 3$\sigma$. *B,* stereoview of interactions of sildenafil (*gold stick-balls*) with the active site residues (*salmon sticks*). The *dotted lines* represent hydrogen bonds. *C,* superposition of sildenafils from the PDE5A1-sildenafil structures of Zhang *et al.* (22) (*gold*), Sung *et al.* (20) (*cyan*), and ours (*green*).

**TABLE 2**
**Interactions of sildenafil and icarisid II with PDE5A**

| Inhibitor | atoms | PDE5 atoms | Distance (Å) |
|---|---|---|---|
| Sildenafil | N4 | Gln817 OE1 | 2.9 |
| | O2 | Gln817 OE1 | 3.2 |
| | O1 | Gln817 NE2 | 3.2 |
| | O1 | $H_2O$ | 2.7 |
| | N1 | $H_2O$ | 2.6 |
| Icarisid II | O1 | Ile768 N | 3.1 |
| | O4 | Ile665 N | 2.8 |
| | O10 | Ser668 OG | 3.0 |
| | O7 | His613 NE2 | 2.7 |
| | O8 | Asp764 OD2 | 2.8 |
| | O8 | $H_2O$ | 2.6 |
| | O10 | $H_2O$ | 2.7 |

Van der Waals' contacts:

| | |
|---|---|
| For sildenafil | |
| Pyrazolopyrimidinone | Tyr612, Leu765, Ala767, Val782, Gln817, Phe820 |
| Ethoxyphenyl | Val782, Ala783, Phe786, Leu804, Ile813, Gln817, Phe820 |
| methylpiperazine | Asn662, Ser663, Tyr664, Ile665, Leu804, Phe820 |
| For icarisid II | |
| Methoxyphenyl | Ala767, Ile768, Gln775, Ala779, Val782, Gln817, Phe820 |
| Oxychromone | Tyr664, Ile665, Ser668, Leu725, Leu804, Met816, Phe820 |
| Pentenyl | Val782, Phe786, Leu804, Met816, Gln817 |
| Rhamnose | Tyr612, His613, Asn661, Ser663, Leu725, Asp764, Leu765, Phe786, Phe820 |

takes the PDE4 conformation because of chimeric replacement of PDE5 residues 658–681 with those of PDE4 (22). Second, the conformations and the interactions of sildenafil in the three PDE5A-sildenafil structures are significantly different. Although the ethoxyphenyl and pyrazolopyrimidinone groups of sildenafil in the three PDE5A structures are superimposable and interact with the same residues of PDE5A, the methylpiperazine shows different orientations (Fig. 3). The methylpiperazine moiety in our PDE5A1-sildenafil structure folds to interact with the pyrazolopyrimidinone, in contrast to the conformation reported by Sung *et al.* (20) where the methylpiperazine extends in a different direction. The orientation of the methylpiperazine in the structure of Zhang *et al.* (22) is more similar to ours, but the ring is tilted by ~40° (Fig. 3). In addition, the contacts between the methylpiperazine and the PDE5 residues in the structure reported herein markedly differ from both previously published structures. In the structure reported herein, the methylpiperazine interacts with $Asn^{662}$, $Ser^{663}$, $Tyr^{664}$, and $Ile^{665}$ in the H-loop (Table 2). However, there are no contacts between the methylpiperazine and the H-loop in the structure of Zhang *et al.* (22), and the methylpiperazine contacts $Tyr^{664}$, $Met^{816}$, $Gly^{819}$, and $Phe^{820}$ in the structure by Sung *et al.* (20).

To exclude possible false results from the structure determination, we compared this study and previously published structures of the PDE5A-sildenafil complex. The $2F_o - F_c$ and $F_o - F_c$ maps that are calculated from the PDE5A catalytic domains with omission of sildenafil show reasonable electron density for all three sildenafils, suggesting their true bound conformations in the crystal states. Thus, the basis for the conformational differences of sildenafil needs to be explored. The 40° tilt of the methylpiperazine ring in the Zhang structure may be the consequence of the chimeric replacement of the PDE5 H-loop (residues 658–681) with the equivalent amino acids of PDE4 (22), which takes the conformation of PDE4 in that structure. For the structure of PDE5A-sildenafil of Sung *et al.* (20), the electron density maps show that $Cys^{677}$ probably forms an intermolecular disulfide bond with $Cys^{677}$ from a neighboring monomer in the PDE5A crystal. Thus, the catalytic domain of PDE5A in the structure of Sung *et al.* (20) forms a dimer, in contrast to a monomeric form in the PDE5A-sildenafil structures of ours and Zhang *et al.* (22). The fact that the specific activity of the catalytic domain of Sung *et al.* (20) is only about one-thousandth of that reported for monomeric PDE5A (see Ref. 40 and this study) suggests that the dimer may be either a less active form of PDE5 or a crystallization artifact.

*Binding of Icarisid II to PDE5*—Icarisid II is a glycoside derivative of flavonoids from the plant *Epimedium wanshanense* that has been used as an herbal medicine for improvement of erectile dysfunction in China for more than a thousand years (41–44). Icarisid II inhibits PDE5A1 with an $IC_{50}$ of 2 $\mu$M and shows at least 10-fold selectivity against other PDEs. It binds to the active site of PDE5A1, as shown by the electron density that is calculated from the PDE5A1 structure before icarisid II was built into the structure (Fig. 4). The binding of icarisid II causes formation of two $\beta$-strands in the H-loop and as much as 35 Å movement of the H-loop to completely close the active site (Figs. 2*E* and 4). The solvent-accessible area of icarisid II after binding to the active site of PDE5A1 is reduced to 0.05% of the unbound form.

Five hydrogen bonds are formed between icarisid II and PDE5A1. The oxychromone ($R_2$, Fig. 1 and Table 2) of icarisid II stacks against $Phe^{820}$, and its oxygen atoms O4 and O10 form three hydrogen bonds with the backbone nitrogen of $Ile^{665}$, the side chain oxygen of $Ser^{668}$, and a water molecule. It also interacts with residues $Tyr^{664}$, $Leu^{725}$, $Leu^{804}$, and $Met^{816}$ (Fig. 4). The methoxyphenyl group ($R_1$, Fig. 1) forms a hydrogen bond with the backbone nitrogen of $Ile^{768}$ and makes van der Waals contacts with $Ala^{767}$, $Ile^{768}$, $Gln^{775}$, $Ala^{779}$, $Gln^{817}$, and $Phe^{820}$ (Table 2). The pentenyl group (atoms C17-C21, Fig. 1) forms hydrophobic contacts with $Val^{782}$, $Phe^{786}$, $Leu^{804}$, $Met^{816}$, and $Gln^{817}$. The rhamnose group ($R_3$, Fig. 1) forms three hydrogen

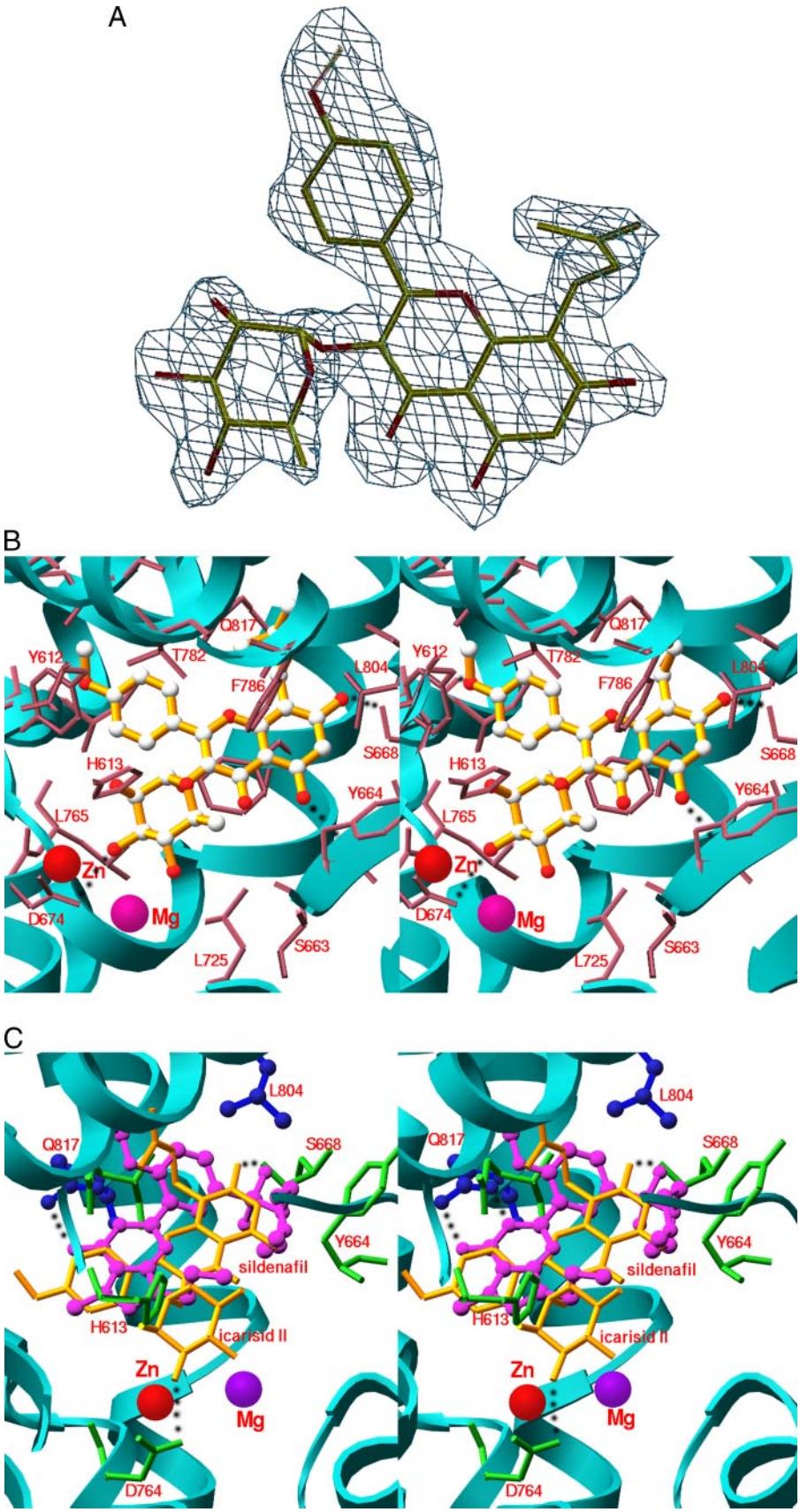


FIGURE 4. **Icarisid II binding.** *A,* electron density for icarisid II bound to PDE5A1. The $F_o - F_c$ map was calculated from the structure with omission of icarisid II and contoured at 3.0$\sigma$. *B,* stereoview of interaction of icarisid II (*gold sticks*) with the PDE5A1 residues (*salmon sticks*) at the active site of PDE5A1. The *dotted lines* represent hydrogen bonds. *C,* superposition of icarisid II (*gold sticks*) and sildenafil (*purple ball-sticks*). Residues from PDE5A-sildenafil are shown in *blue,* and residues from the icarisid II complex are in *green.* The side chain of $Gln^{817}$ has the different conformations in the two structures.

**TABLE 3**
**Kinetic properties of PDE5A1-(535–860) isolated catalytic domain and its mutants**

| | $K_m^{cGMP}$ | $k_{cat}^{cGMP}$ | $(k_{cat}/K_m)^{cGMP}$ | IBMX | Icarisid II | Sildenafil |
|---|---|---|---|---|---|---|
| | $\mu M$ | $s^{-1}$ | $s^{-1}\ \mu M^{-1}$ | $IC_{50}\ \mu M$ | $IC_{50}\ \mu M$ | $IC_{50}\ nM$ |
| Wild type | 5.1 ± 1.3 | 1.3 ± 0.3 | 0.27 ± 0.08 | 2.1 ± 0.5 | 1.7 ± 0.4 | 2.4 ± 0.3 |
| Δ(663–678)[a] | 54 ± 6 | 3.8 ± 0.5 | 0.07 ± 0.013 | 5.3 ± 1.1 | 2.5 ± 0.2 | 5.9 ± 1.5 |
| Δ(661–681)[a] | 750 ± 210 | 2.3 ± 0.6 | 0.0031 ± 0.0002 | 95 ± 6 | 55 ± 13 | 188 ± 29 |

[a] Four glycines were inserted as a linker. Each of the experiments was repeated three times.

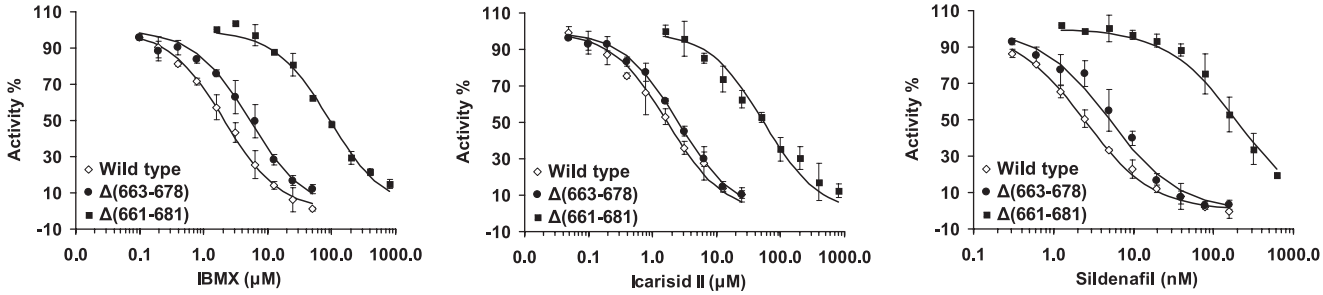


FIGURE 5. **Inhibition of the isolated PDE5 catalytic domain of wild type and H-loop deletion mutants by IBMX, icarisid II, and sildenafil.**

**TABLE 4**
**Kinetic properties of full-length wild type PDE5A1 and PDE5A1 mutant proteins**

| | $K_m^{cGMP}$ | $(k_{cat}/K_m)^{cGMP}$ | $(k_{cat}/K_m)^{cGMP}$ |
|---|---|---|---|
| | $\mu M$ | $s^{-1}$ | $s^{-1}\ \mu M^{-1}$ |
| Wild type | 2.95 ± 0.81 | 1.67 ± 0.31 | 0.57 |
| G659A | 71.20 ± 1.22 | 0.112 ± 0.00013 | 0.0016 |
| V660Q | 82.06 ± 8.46 | 2.53 ± 0.71 | 0.031 |
| N661A | 68.06 ± 4.32 | 0.86 ± 0.04 | 0.013 |
| N662A | 15.15 ± 1.92 | 0.18 ± 0.10 | 0.012 |
| Y664A | 80.36 ± 8.76 | 1.51 ± 0.35 | 0.019 |
| H678A | 3.87 ± 0.10 | 0.53 ± 0.06 | 0.14 |
| S679A | 70.28 ± 5.45 | 1.83 ± 0.37 | 0.026 |

bonds with Nϵ2 of $His^{613}$, Oδ2 of $Asp^{764}$, and a water molecule, in addition to interactions with residues $Tyr^{612}$, $His^{613}$, $Asn^{661}$, $Ser^{663}$, $Leu^{725}$, $Asp^{764}$, $Leu^{765}$, and $Phe^{820}$ (Table 2). A few atoms of rhamnose are located at distance suitable for van der Waals contact with both metal ions and directly interact with some of the metal-binding residues such as $Asp^{764}$.

Although icarisid II and sildenafil occupy the same active site, the detailed interactions of the inhibitors are significantly different (Fig. 4). Sildenafil forms two hydrogen bonds with $Gln^{817}$ and stacks against $Phe^{820}$. However, $Gln^{817}$ shows about 90° rotation of its side chain (Fig. 4) and forms no hydrogen bond with icarisid II. The hydrogen bond between the side chain atoms of Oϵ1 of $Gln^{775}$ and Nϵ2 of $Gln^{817}$ in the unliganded PDE5 and its complex with IBMX and sildenafil vanishes in the PDE5-icarisid II structure, and the two atoms separate by 4.3 Å. The conformational change of the side chain $Gln^{817}$ in the icarisid II structure appears to be a consequence of its unfavorable proximity to the hydrophobic pentenyl and phenyl groups. In addition, the position of oxychromone of icarisid II, which stacks against $Phe^{820}$, is significantly different from the pyrazolopyrimidinone of sildenafil. In consideration of the 1000-fold difference in binding affinity between sildenafil and icarisid II, the structural data suggest that the hydrogen bond with $Gln^{817}$ and the stacking against $Phe^{820}$ are two essential components for high affinity binding of inhibitors. This result is consistent with an established role of $Gln^{817}$ in providing for high potency of sildenafil, vardenfil, and tadalafil (45).

*A Potential Role of the H-loop in Substrate/Inhibitor Recognition*—To understand the biochemical basis of multiple conformations of the H-loop, two deletion mutants were created in the isolated catalytic domain of PDE5A1. The PDE5A1 mutant with deletion of residues 663–678 and insertion of four glycines (to minimize perturbation of the structure) showed about 10- and 2-fold lower affinity for cGMP and the inhibitors, respectively (Table 3 and Fig. 5). The mutant protein in which residues 661–681 had been deleted and four glycines had been inserted had a 150-fold weaker $K_m$ value for cGMP and 30–80-fold less potent $IC_{50}$ value for the inhibitors (Table 3). However, both mutants had $k_{cat}$ values comparable with that of the wild type PDE5A1 catalytic domain. These data imply that the H-loop has a very important role for interaction of PDE5A1 with the cGMP substrate but appears to be less critical in interaction with icarisid II or sildenafil than with cGMP. This is consistent with an earlier report that a sildenafil homolog UK-122764 that lacks methylpiperazine and thus interactions with the H-loop shows only a 5-fold lower potency than sildenafil (46).

To pinpoint residues that impact cGMP binding affinity, single mutations were performed on selected H-loop residues ($Val^{660}$, $Asn^{661}$, $Asn^{662}$, $Tyr^{664}$, $His^{678}$, and $Ser^{679}$) in full-length human PDE5A1, in addition to $Gly^{659}$, an invariant amino acid among all class I PDEs. Mutation of $Gly^{659}$ to alanine (G659A) caused a 17-fold loss of $k_{cat}$ and 24-fold weaker affinity for cGMP (Table 4). The N662A mutant exhibited a modest loss (5-fold) in affinity for cGMP and a 9-fold decrease in $k_{cat}$. Mutation of H678A did not appreciably impact the binding affinity of substrate or catalytic activity. The remaining mutations (V660Q, N661A, Y664A, and S679A) did not significantly change $k_{cat}$ but caused a 24–28-fold loss in affinity for cGMP (Table 4). To verify the overall structural integrity of the full-length PDE5A1 constructs, cGMP binding to the allosteric cGMP sites in the regulatory domain of each mutant was assessed. Wild type and mutant PDE5A1 proteins bound cGMP with comparable affinity ($K_d$ in the range of 190–230 nM) and stoichiometry (0.50–0.55 mol of cGMP per PDE5A1 monomer), in good agreement with values reported previously for

recombinant bovine PDE5 (40). These data indicate that overall structures of the mutant proteins are preserved and that differences in kinetic parameters for the mutants are not because of nonspecific conformational effects.

Properties of the G659A mutant can be explained on basis of the PDE structures. $Gly^{659}$ is invariant in all class I PDE families, immediately precedes the H-loop, and is likely to provide critical flexibility at this juncture in the protein structures. $Gly^{659}$ has backbone conformational angles of $\phi = 76–105°$, $\varphi = 3–22°$, and $\omega = \sim 180°$ in the structures of PDE5A1-sildenafil, PDE5A1-icarisid II, and other PDE families, and $\phi = 104–109°$, $\varphi = 139–141°$, and $\omega = \sim 180°$ in the unliganded and IBMX-bound PDE5A1. All of these $\phi/\varphi$ conformational angles are allowed only for glycine but are not allowed for all other amino acids. Thus, mutation of $Gly^{659}$ to any other amino acid would impose restrictions on the conformation of the H-loop or even distort the conformation of the active site, thus profoundly impairing the catalytic activity of the mutant PDE5.

The kinetic data indicate that the majority of the H-loop mutants affect $K_m$ values for cGMP but have much less effect in catalytic turnover rate (Table 4). Although no interactions between the H-loop and the low affinity product GMP were observed in the chimeric PDE5-GMP structure (22), it is plausible that the H-loop may contact cGMP in a pattern like that of sildenafil or icarisid II. Because hydrolysis of the phosphodiester bond of cGMP occurs in the metal-binding subpocket, the distal position of the H-loop from the metal site in the structure would be more consistent with its role in substrate binding rather than hydrolysis. This would imply a dynamic interplay between the H-loop and substrate, in which binding of cGMP and the H-loop conformation would mutually regulate one another. Further structural studies will be required to completely define the mechanism involved in the H-loop modulation of substrate affinity and inhibitor binding.

## DISCUSSION

Extensive studies on the crystal structures of PDEs have shown that the PDE families have similar overall three-dimensional structures for their isolated catalytic domains and active sites (20–25, 32–39). However, information on the conformation of the PDE5 active site and on sildenafil binding is incomplete because early studies showed a disordered or artificially replaced H-loop at the active site (20–22). This study, in combination with our PDE5A1-IBMX structure (23), reveals that the H-loop of PDE5 can adopt four clearly defined conformations. These different conformations of the H-loop of PDE5 may be the result of direct contacts between the H-loop and inhibitors, such as those in the structures of PDE5A1 in complex with sildenafil or icarisid II. Alternatively, the H-loop changes may be imposed by more distant effects of conformational changes following inhibitor occupation of the binding pocket, as implicated by no direct contacts between the H-loop and IBMX. Finally, a combination of both direct and indirect interactions may contribute to the H-loop changes. Because all other PDEs appear to have a similar conformation of the H-loop that is not comparable with any of the conformations of the PDE5 H-loop, the PDE5 active site apparently has a unique structural characteristic. The mutual communication between inhibitor binding and conformational changes of the PDE5 catalytic pocket may thus be a valuable consideration for design of new inhibitors with unique selectivity against PDE5.

It is common that an inhibitor slightly adjusts its conformation to provide an optimal fit in the binding pocket of a protein. However, the conformational variation of sildenafil in the different crystal forms, as seen in the significantly different conformations of the methylpiperazine group, is unusual. Because inhibitors are commonly designed to mimic contacts employed by the substrate, the dramatic effect of the H-loop mutations on affinity for cGMP and the flexibility of sildenafil provide potentially important direction in development of new PDE5 inhibitors.

Side effects such as visual disturbances in patients who ingest PDE5 inhibitors (19) dictate a need for detailed study of the molecular basis for the action of these drugs and development of new potential inhibitors. Derivatives of flavonoids such as icarasid II may be such a new category of PDE5 inhibitors. Flavonoids inhibit PDEs with affinity at the micromolar level and slight selectivity (47, 48), and are widely used as dietary supplements that have reached a multiple billion dollar business (49–51). In the present report, the structure of PDE5A1-icarisid II shows how this natural dietary compound interacts with PDE5 and thus provides a valuable guideline for development of a new category of PDE5 inhibitors.

*Acknowledgment—We thank the National Synchrotron Light Source for collection of diffraction data. We especially thank Drs. Kenji Omori and Jun Kotera of Tanabe-Seiyaku Pharmaceutical Co. Ltd. (Saitama, Japan) for kindly providing human PDE5A1 cDNA. We also thank Meiyan Zheng and Kennard Grimes for their excellent technical assistance.*

## REFERENCES

1. Manganiello, V. C., Taira, M., Degerman, F., and Belfrage, P. (1995) *Cell. Signal.* **7,** 445–455
2. Houslay, M. D., Sullivan, M., and Bolger, G. B. (1998) *Adv. Pharmacol.* **44,** 225–343
3. Torphy, T. J. (1998) *Am. J. Respir. Crit. Care Med.* **157,** 351–370
4. Soderling, S. H., and Beavo, J. A. (2000) *Curr. Opin. Cell Biol.* **12,** 174–179
5. Francis, S. H., Turko, I. V., and Corbin, J. D. (2001) *Prog. Nucleic Acids Res. Mol. Biol.* **65,** 1–52
6. Mehats, C., Andersen, C. B., Filopanti, M., Jin, S. L., and Conti, M. (2002) *Trends Endocrinol. Metab.* **13,** 29–35
7. Conti, M., Richter, W., Mehats, C., Livera, G., Park, J. Y., and Jin, C. (2003) *J. Biol. Chem.* **278,** 5493–5496
8. Houslay, M. D., and Adams, D. R. (2003) *Biochem. J.* **370,** 1–18
9. Goraya, T. A., and Cooper, D. M. (2005) *Cell. Signal.* **17,** 789–797
10. Movsesian, M. A. (2000) *Exp. Opin. Investig. Drugs* **9,** 963–973
11. Truss, M. C., Stief, C. G., Uckert, S., Becker, A. J., Wafer, J., Schultheiss, D., and Jonas, U. (2001) *World J. Urol.* **19,** 344–350
12. Liu, Y., Shakur, Y., Yoshitake, M., and Kambayashi, J. J. (2001) *Cardiovasc. Drug Rev.* **19,** 369–386
13. Huang, Z., Ducharme, Y., MacDonald, D., and Robinchaud, A. (2001) *Curr. Opin. Chem. Biol.* **5,** 432–438
14. Rotella, D. P. (2002) *Nat. Rev. Drug Discovery* **1,** 674–682
15. Corbin, J. D., and Francis, S. H. (2002) *Int. J. Clin. Pract.* **56,** 453–459
16. Lipworth, B. J. (2005) *Lancet* **365,** 167–175
17. Castro, A., Jerez, M. J., Gil, C., and Martinez, A. (2005) *Med. Res. Rev.* **25,** 229–244

18. Galie, N., Ghofrani, H. A., Torbicki, A., Barst, R. J., Rubin, L. J., Badesch, D., Fleming, T., Parpia, T., Burgess, G., Branzi, A., Grimminger, F., Kurzyna, M., and Simonneau, G. (2005) *N. Engl. J. Med.* **353,** 2148–2157
19. Pomeranz, H. D., and Bhavsar, A. R. (2005) *J. Neuroophthalmol.* **25,** 9–13
20. Sung, B. J., Hwang, K. Y., Jeon, Y. H., Lee, J. I., Heo, Y. S., Kim, J. H., Moon, J., Yoon, J. M., Hyun, Y. L., Kim, E., Eum, S. J., Park, S. Y., Lee, J. O., Lee, T. G., Ro, S., and Cho, J. M. (2003) *Nature* **425,** 98–102
21. Brown, D. G., Groom, C. R., Hopkins, A. L., Jenkins, T. M., Kamp, S. H., O'Gara, M. M., Ringrose, H. J., Robinson, C. M., and Taylor, W. E. (May 8, 2003) WIPO Patent WO 03/2003/038080
22. Zhang, K. Y., Card, G. L., Suzuki, Y., Artis, D. R., Fong, D., Gillette, S., Hsieh, D., Neiman, J., West, B. L., Zhang, C., Milburn, M. V., Kim, S. H., Schlessinger, J., and Bollag, G. (2004) *Mol. Cell* **15,** 279–2861
23. Huai, Q., Liu, Y., Francis, S. H., Corbin, J. D., and Ke, H. (2004) *J. Biol. Chem.* **279,** 13095–13101
24. Card, G. L., England, B. P., Suzuki, Y., Fong, D., Powell, B., Lee, B., Luu, C., Tabrizizad, M., Gillette, S., Ibrahim, P. N., Artis, D. R., Bollag, G., Milburn, M. V., Kim, S. H., Schlessinger, J., and Zhang, K. Y. (2004) *Structure* (*Camb.*) **12,** 2233–2247
25. Wang, H., Liu, Y., Chen, Y., Robinson, H., and Ke, H. (2005) *J. Biol. Chem.* **280,** 30949–30955
26. Thomas, M. K., Francis, S. H., and Corbin, J. D. (1990) *J. Biol. Chem.* **265,** 14971–14978
27. Otwinowski, Z., and Minor, W. (1997) *Methods Enzymol.* **276,** 307–326
28. Navaza, J., and Saludjian, P. (1997) *Methods Enzymol.* **276,** 581–594
29. Collaborative Computational Project, Number 4 (1994) *Acta Crystallogr. Sect. D Biol. Crystallogr.* **50,** 760–763
30. Jones, T. A., Zou, J.-Y., Cowan, S. W., and Kjeldgaard, M. (1991) *Acta Crystallogr. Sect. A* **47,** 110–119
31. Brünger, A. T., Adams, P. D., Clore, G. M., DeLano, W. L., Gros, P., Grosse-Kunstleve, R. W., Jiang, J. S., Kuszewski, J., Nilges, M., Pannu, N. S., Read, R. J., Rice, L. M., Simonson, T., and Warren, G. L. (1998) *Acta Crystallogr. Sect. D Biol. Crystallogr.* **54,** 905–921
32. Iffland, A., Kohls, D., Low, S., Luan, J., Zhang, Y., Kothe, M., Cao, Q., Kamath, A. V., Ding, Y. H., and Ellenberger, T. (2005) *Biochemistry* **44,** 8312–8325
33. Scapin, G., Patel, S. B., Chung, C., Varnerin, J. P., Edmondson, S. D., Mastracchio, A., Parmee, E. R., Singh, S. B., Becker, J. W., Van der Ploeg, L. H., and Tota, M. R. (2004) *Biochemistry* **43,** 6091–6100
34. Xu, R. X., Hassell, A. M., Vanderwall, D., Lambert, M. H., Holmes, W. D., Luther, M. A., Rocque, W. J., Milburn, M. V., Zhao, Y., Ke, H., and Nolte, R. T. (2000) *Science* **288,** 1822–1825
35. Xu, R. X., Rocque, W. J., Lambert, M. H., Vanderwall, D. E., Luther, M. A., and Nolte, R. T. (2004) *J. Mol. Biol.* **337,** 355–365
36. Lee, M. E., Markowitz, J., Lee, J. O., and Lee, H. (2002) *FEBS Lett.* **530,** 53–58
37. Huai, Q., Wang, H., Sun, Y., Kim, H. Y., Liu, Y., and Ke, H. (2003) *Structure* (*Camb.*) **11,** 865–873
38. Huai, Q., Colicelli, J., and Ke, H. (2003) *Biochemistry* **42,** 13220–13226
39. Huai, Q., Wang, H., Zhang, W., Colman, R., Robinson, H., and Ke, H. (2004) *Proc. Natl. Acad. Sci. U. S. A.* **101,** 9624–9629
40. Fink, T. L., Francis, H., Beasley, A., Grimes, K. A., and Corbin, J. D. (1999) *J. Biol. Chem.* **274,** 24613–24620
41. Li, W. K., Zhang, R. Y., and Xiao, P. G. (1996) *Phytochemistry* **43,** 527–530
42. Kuroda, M., Mimaki, Y., Sashida, Y., Umegaki, E., Yamazaki, M., Chiba, K., Mohri, T., Kitahara, M., Yasuda, A., Naoi, N., Xu, Z. W., and Li, M. R. (2000) *Planta Med.* **66,** 575–577
43. Xin, Z., Kim, E., Tian, Z., Lin, G., and Guo, Y. (2001) *Chin. Sci. Bull.* **46,** 1186–1190
44. Xin, Z., Kim, E. K., Lin, C. S., Liu, W. J., Tian, L., Yuan, Y. M., and Fu, J. (2003) *Asian J. Androl.* **5,** 15–18
45. Zoraghi, R., Corbin, J. D., and Francis, S. H. (2006) *J. Biol. Chem.* **281,** 5553–5558
46. Turko, I. V., Ballard, S. A., Francis, S. H., and Corbin, J. D. (1999) *Mol. Pharmacol.* **56,** 124–130
47. Nichols, M. R., and Morimoto, B. H. (2000) *Mol. Pharmacol.* **57,** 738–754
48. Ko, W., Shih, C., Lai, Y., Chen, J., and Huang, H. (2004) *Biochem. Pharmacol.* **68,** 2087–2094
49. Barnes, S., Boersma, B., Patel, R., Kirk, P. M., Darley-Usmar, V. M., Kim, H., and Xu, J. (2000) *Biofactors* **12,** 209–215
50. Fitzpatrick, L. A. (2003) *Maturitas* **44,** S21–S29
51. Limer, J., and Speirs, V. (2004) *Breast Cancer Res.* **6,** 119–127